Supplementary Information

Efficient Growth and Characterization of One-dimensional Transition Metal Tellurides Inside Carbon Nanotubes

Naoyuki Kanda,[a,b] Yusuke Nakanishi,[*a] Dan Liu,[c,d] Zheng Liu,[e] Tsukasa Inoue,[b] Yasumitsu Miyata,[a] David Tománek,[c] and Hisanori Shinohara[b]

[a.] *Department of Physics, Tokyo Metropolitan University, Tokyo 192-0397, Japan.*

[b.] *Department of Chemistry, Nagoya University, Nagoya 464-8602, Japan.*

[c.] *Department of Physics and Astronomy, Michigan State University, East Lansing, Michigan 48824, United States.*

[d.] *Theoretical Division, Physics and Chemistry of Materials, Los Alamos National Laboratory, Los Alamos, New Mexico 87545, United States.*

[e.] *National Institute of Advanced Industrial Science and Technology (AIST), Nagoya 463-8560, Japan.*

Address correspondence to:

naka24ysk@gmail.com (Y.N.)

Materials & Methods

Preparation of MoTeNWs. High-quality arc-discharge CNTs (Meijo Nano Carbon Co. Ltd.) were employed as templates for the NWs formation. Closed ends of CNTs were opened by an oxidation treatment, during which the temperature is increased to 500 °C in 6h in air. The as-prepared CNTs were degassed for 1h under a vacuum of 10^{-7} Torr. Typically, 0.3 mg of the open-ended CNTs was sealed in a straight quartz tube under vacuum (10^{-7} Torr) with 3 mg of MoO_2 and 3 mg of Te, and then heated at 1100 °C for 48h.

Preparation of WTeNWs. Typically, 0.3 mg of the open-ended CNTs was sealed in a straight quartz tube under vacuum (10^{-7} Torr) with 1.5 mg of WO_3 and 3 mg of Te, and then heated at 900 °C for 48h.

Raman Spectroscopy. Raman scattering measurement was carried out by means of the invia confocal Raman systems equipped with a microscope (HORIBA JOBIN Yvon). The

laser spot size was ϕ4 μm and the laser power was 400 μW. The excitation wavelength was 633 nm (He-Ne Laser).

C_s-corrected STEM observation. C_s-corrected HAADF-STEM images were taken by using a JEM-ARM200F ACCELARM (cold FEG) equipped with a CEOS C_s corrector (ASCOR system), operated at 120 keV. The scan rate was 38 microseconds (38 μs) per pixel.

XPS Spectroscopy. XPS analyses were performed by using an ESCALAB 250Xi (Thermo Fisher Scientific Inc.) by using monochromatic Al X-ray source. Instrument-base pressure was 7×10^{-10} Torr. High-resolution XPS spectra were collected using an analysis 650 μm in diameter and 50 eV pass energy. Charge neutralization system was employed for all analyses by flood gun with Ar gas.

Absorption Spectroscopy. Optical absorption spectra were measured on Shimadzu UV-3600 spetrophotometer with a path of 10 mm.

DFT Simulations. We have investigated the equilibrium geometry and structural stability of a series of molecules including molybdenum oxides, tellurium oxide TeO_2, and Mo_xTe_x (x=3,6,9). The interaction between MoO_2 and graphene was calculated using *ab initio* DFT as implemented in the VASP code.[1-3] We studied these molecules in a periodic array separated by a vacuum region in excess of 25 Å. The 2D system of MoO_2 on graphene was represented by a periodic array of layers separated by a vacuum region of >20 Å. We employed projector-augmented wave (PAW) pseudopotentials[4,5] and the Perdew−Burke−Ernzerhof (PBE) exchange-correlation functional.[6] The Brillouin zone of the conventional unit cell of 0D and 2D structures has been sampled by a uniform k-point grid.[7] The specific sampling was 1×1×1 for isolated molecule optimization, and 3×3×1 for MoO_2 on graphene. We employed 600 eV as the electronic kinetic energy cutoff for the plane-wave basis and a total energy difference between subsequent self-consistency iterations below 10^{-5} eV/atom as the criterion for reaching self-consistency. All the geometries have been optimized using the conjugate-gradient method,[8] until none of the residual Hellmann−Feynman forces exceeded 10^{-2} eV/Å.

2. Optimization of the reaction temperature

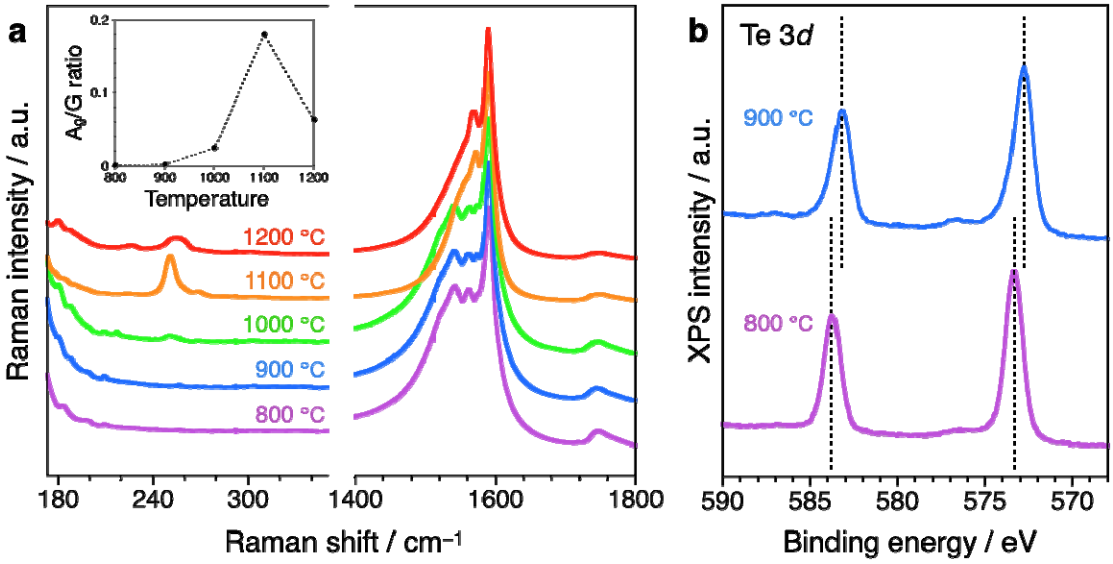

Fig. S1 (a) Raman spectra of the products annealed at different temperatures (800–1200 °C), excited at the laser wavelengths of 633 nm. Inset shows the relative Raman intensity at 251 cm^{-1}, which is defined as the ratio of Raman intensity at 251 cm^{-1} (due to A_g mode of MoTeNWs) to G-band of CNTs at 1583 cm^{-1}, plotted as a function of annealing temperature. (b) XPS Te-3*d* core-levels spectra of the products obtained at 800 and 900 °C.

The formation of MoTeNWs is strongly dependent on the annealing temperature. Raman spectroscopy was performed on the products, which were annealed at a series of different temperatures (Fig. S1a). The Raman signal at 251 cm^{-1} associated with A_g mode of MoTeNWs arises as the starting materials are annealed in vacuum above 900 °C. As shown in the inset of Fig. S1a, the intensity of this Raman feature (relative intensity of this peak to G-band of CNTs) increases with increasing temperature and reaches its maximum at 1100 °C, and decreases with the decomposition of the NWs above the temperatures (~1200 °C). The temperature dependence of the Raman signal suggests that annealing of the reactants at 1100 °C produces MoTeNWs in high yield. Further XPS analysis supported that the evolution of chemical reactions occurs between 800 and 900 °C. As displayed in Figure S1b, XPS spectrum of the products obtained at 900 °C show the Te-3$d_{5/2}$ and Te-3$d_{3/2}$ peaks at binding energies of 572.6 and 583.0 eV, which are attributable to the formation of MoTeNWs inside CNTs. Compared to 900 °C, a 0.8 eV blueshift was observed at 800 °C. The shifted peak can be assigned to pure Te, suggesting that TeNWs are predominantly formed inside CNTs.

3. Chemical analysis by means of XPS and EDS

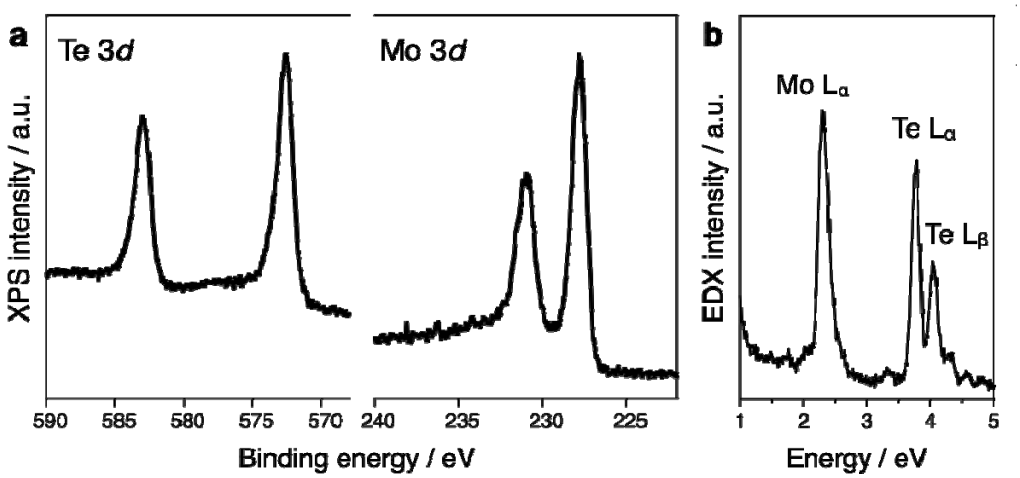

Fig. S2 (a) XPS and (b) EDS spectra of MoTeNWs inside CNTs. As displayed in Figure S2a, Mo-3*d* and XPS Te-3*d* core-levels spectra of the present products show the Mo-$3d_{5/2}$, Mo-$3d_{3/2}$, Te-$3d_{5/2}$, and Te-$3d_{3/2}$ peaks at binding energies of 227.8, 231.0, 572.6 and 583.0 eV, respectively. The binding energies are in accordance with the values of the previously reported MoTeNWs encapsulated inside CNTs.[9] Quantitative chemical analyses by means of EDS yields 1:1 atomic ratio of Mo and Te.

4. Quantitative Raman Spectroscopy

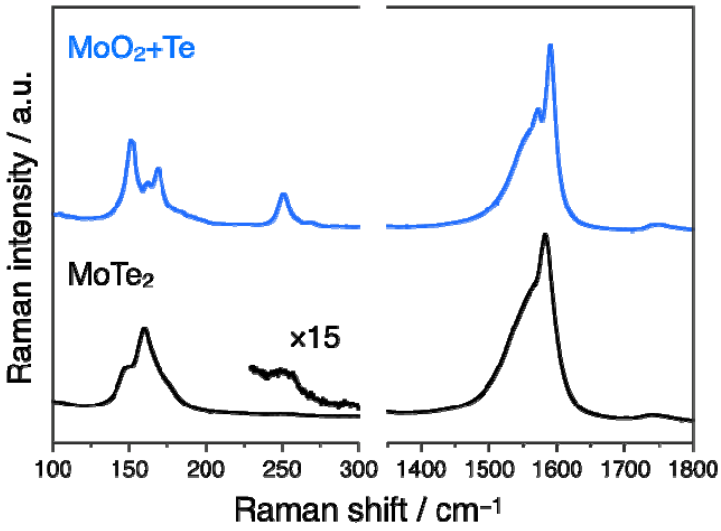

Fig. S3 Expanded Raman spectra of the products obtained *via* vacuum annealing of the mixture of MoO_2 and Te (blue) and bulk $MoTe_2$ crystals (black). Notice that these two starting materials contain the same amount of Mo atoms (0.023 mmol). The sample preparations were carried out under the same conditions (10^{-7} Torr, 1100 °C for 48h).

5. Additional Results of DFT Calculations

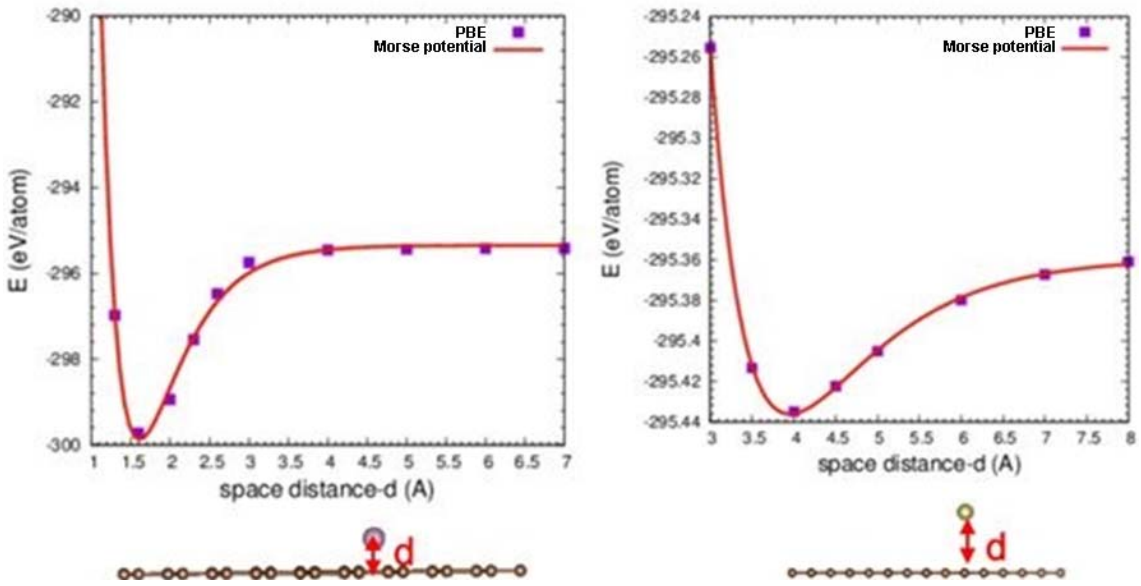

Fig. S4 Stabilization energy and equilibrium geometry of (left) Mo and (right) Te atoms adsorbed on graphene as a function of the separation *d*.

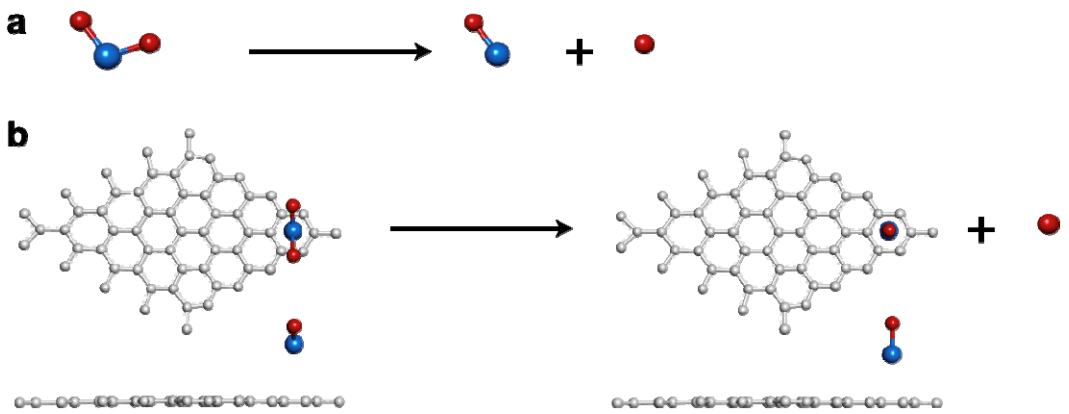

Fig. S5 Breaking the Mo–O bond of the MoO_2 molecule (a) in free space and (b) on graphene.

In order to figure out the effect of CNTs on the chemical reactions, we have calculated the dissociation energy for a bond Mo–O in MoO_2 molecule without and with a graphene sheet (Fig. S5). All the geometries were fully optimized within appropriate symmetry constraints. The energy which is needed to break the Mo–O bond through the reaction shown in Figure S5a is estimated to be 9.684 eV. On the other hand, the Mo–O dissociation energy for MoO_2 molecule attached on the

graphene is lowered to 7.747 eV. In the optimized structures in Fig. S5b, the Mo atom faces graphene and transfers 0.236 electrons to the sheet. As a consequence, the energy needed to break Mo–O bond is significantly reduced.

6. Further STEM information

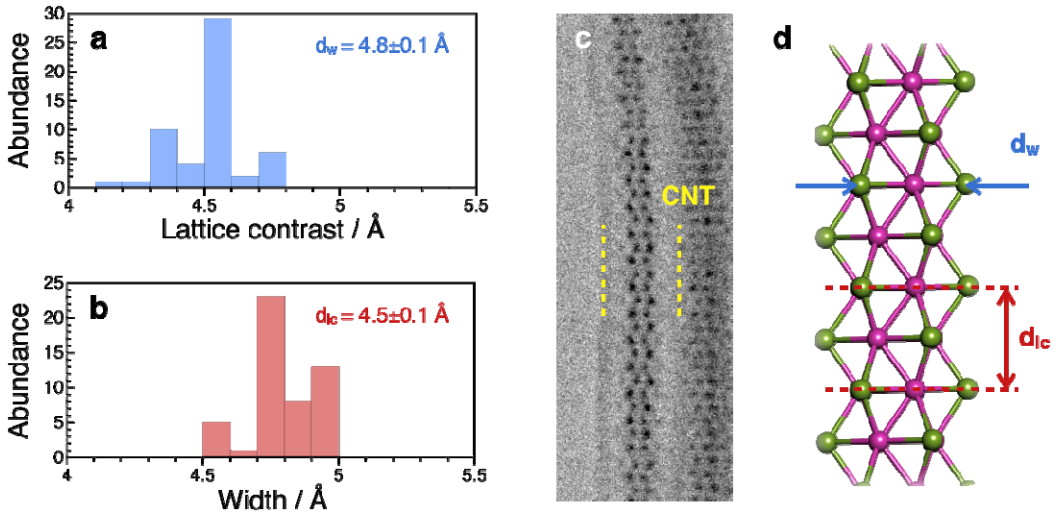

Fig. S6 Distribution of (a) widths and (b) lattice parameters in WTeNWs. (c) A representative C_s-corrected TEM image and (d) atomic structure of an individual WTeNW confined within CNTs.

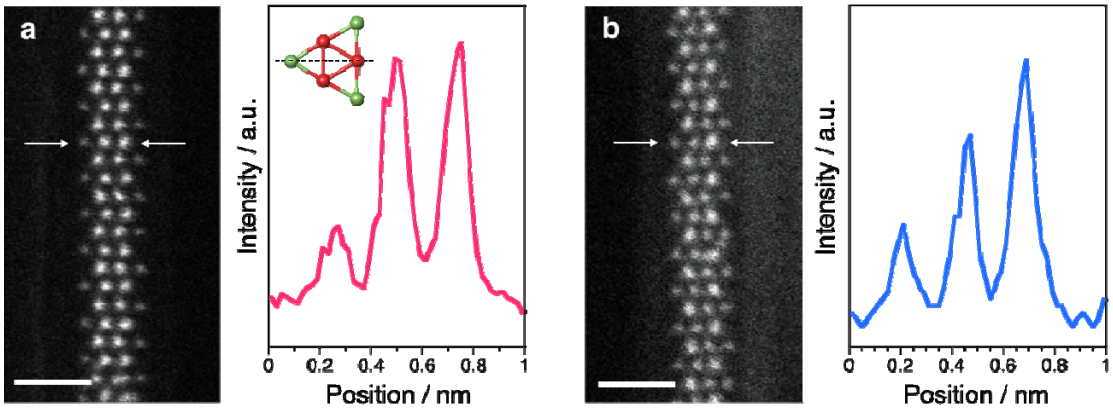

Fig. S7 Typical HAADF-STEM images of (a) WTe- and (b) MoTeNWs confined within CNTs and line intensity profiles along the *X-X'* and *Y-Y'* directions in the corresponding images, respectively. Scale bar, 1 nm.

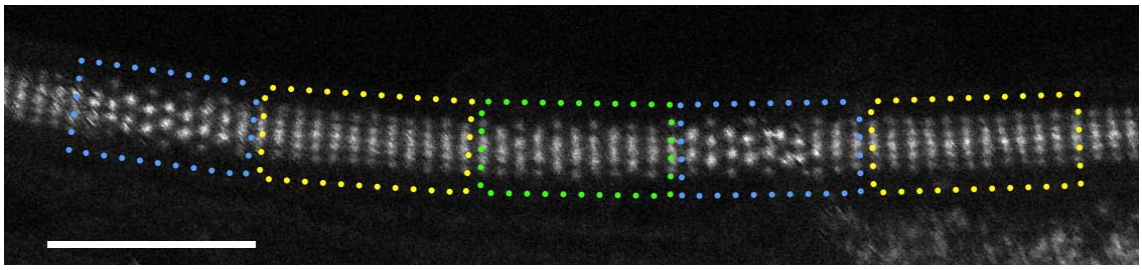

Fig. S8 Torsional motions of an individual WTeNW confined within CNTs. Scale bar, 3 nm.

7. Raman signals of MoTe- and WTeNWs confined in CNTs

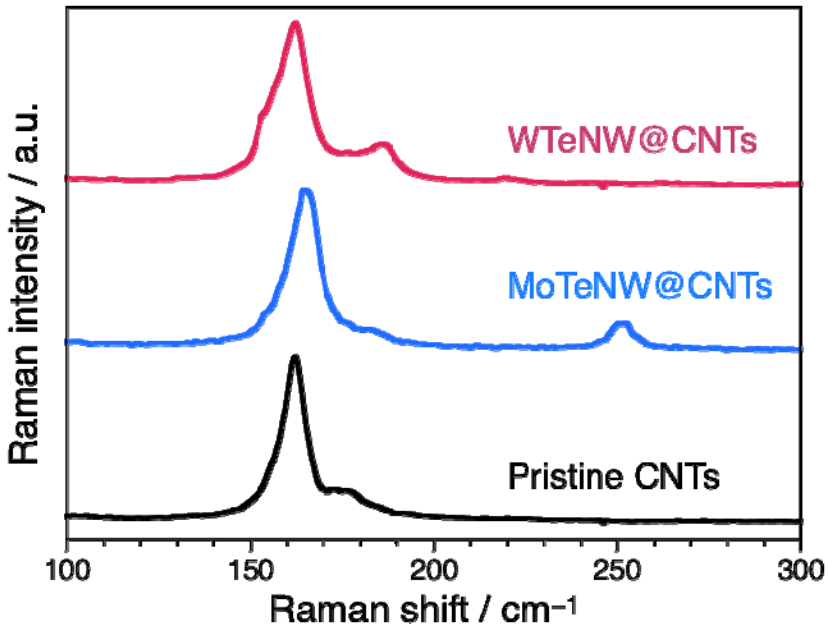

Fig. S9 Raman spectra of WTeNWs@CNT (pink), MoTeNW@CNTs (blue) and pristine CNTs (black).

References

1. G. Kresse and J. Furthmüller, *Phys. Rev. B* 1996, **54**, 11169–11186.
2. G. Kresse and J. Furthmüller, *Comput. Mater. Sci.* 1996, **6**, 15–50.
3. G. Kresse and J. Hafner, *Phys. Rev. B* 1994, **49**, 14251–14269.
4. P. E. Blöchl, *Phys. Rev. B* 1994, **50**, 17953.
5. G. Kresse and D. Joubert, *Phys. Rev. B* 1999, **59**, 1758.
6. J. P. Perdew, K. Burke, and M. Ernzerhof, *Phys. Rev. Lett.* 1996, **77**, 3865–3868.
7. H. J. Monkhorst and J. D. Pack, *Phys. Rev. B* 1976, **13**, 5188.
8. M. R. Hestenes and E. Stiefel, *J. Res. Natl. Bur. Stand.* 1952, **49**, 409–436.
9. M. Nagata, S. Shukla, Y. Nakanishi, Z. Liu, Y.-C. Lin, T. Shiga, Y. Nakamura, T. Koyama, H. Kishida, T. Inoue, *et al.*, *Nano Lett.* 2019, **19**, 4845–4851.